9 Special Waveguide Types

9.1 INTRODUCTION

The preceding chapter dealt with the important special case of waveguides with cylindrical conducting boundaries. In this chapter, we examine several examples of waveguiding systems of different shapes and properties.

We start with dielectric guides which demonstrate that boundaries other than metal–dielectric boundaries can guide waves in cylindrical systems. Dielectric guides are now important for optical communication uses and are explored more in Chapter 14. There follows an examination of radial guiding, both in cylindrical coordinates and in spherical coordinates. The former is important in certain classes of resonant systems and the latter in antenna theory. Waveguides of special cross section, used either for impedance matching or to lower the cutoff frequency for a given transverse dimension, are analyzed. Finally, classes of waves with phase velocity much slower than the velocity of light are studied both in uniform systems and in periodic systems. These are important for such purposes as the interaction with electron beams in traveling-wave tubes and for confining electromagnetic energy near a surface.

The examples selected are not only important in themselves but illustrate a number of important principles. The principle of duality shows how the solution of one problem may sometimes be used for another by interchange of electric and magnetic fields. Cutoff in a waveguide is shown to correspond to a condition of transverse resonance, which leads to a variety of approximate and exact techniques for analyzing guides of irregular shape. Periodic systems show the importance of spatial harmonics for interpreting the behavior of such systems.

9.2 DIELECTRIC WAVEGUIDES

Dielectric rods, slabs, or films can guide electromagnetic energy if surrounded by a dielectric of lower permittivity. Guides of this type were analyzed by Hondros and

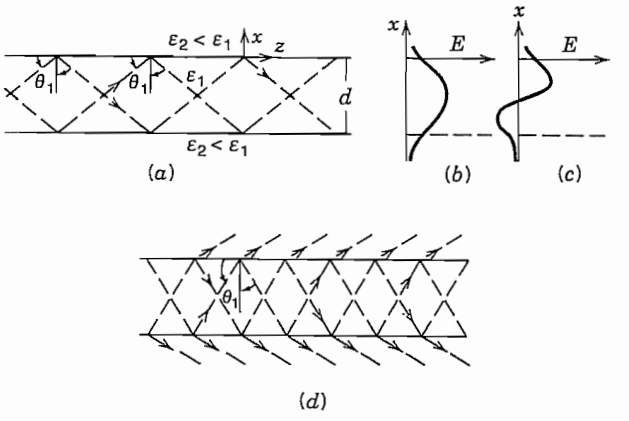

FIG. 9.2 (*a*) Rays totally reflected from dielectric boundaries when $\varepsilon_1 > \varepsilon_2$ and $\theta_1 > \theta_c$. (*b*) Form of electric field distribution versus x in lowest-order mode. (*c*) Form of field versus x in next higher-order mode. (*d*) Leaky wave when $\theta_1 < \theta_c$.

Debye[1] in 1910 and demonstrated by Zahn[2] in 1916. They have become very important as guides for light in optical communication systems, and so will be treated in detail in Chapter 14. Because of the importance of the principle and some use in other frequency ranges, we introduce the subject here with some physical pictures and comparisons with metal-clad guiding systems.

To illustrate dielectric guiding, consider the slab guide of Fig. 9.2*a* with dielectric ε_1 surrounded by $\varepsilon_2 < \varepsilon_1$. In this picture we consider the mode as made up of plane waves reflecting at an angle from the boundaries between dielectrics, interfering within the slab to produce a particular mode pattern when conditions are correct.[3] From the concept of total reflection (Sec. 6.12), we know that all energy is reflected from the interface if angle θ_1 of the rays (normals to the wavefronts) is greater than critical angle θ_c,

$$\theta_c = \sin^{-1}(\varepsilon_2/\varepsilon_1)^{1/2} \tag{1}$$

where we assume $\mu_1 = \mu_2$. The interference within the slab to produce a mode pattern is analogous to that described for the TE_{10} mode of rectangular guide (Sec. 8.8). The differences are in the phases of reflections at the boundaries and in the evanescent fields extending into the dielectric regions above and below the dielectric guide.

The exponential decay of fields in the dielectric of region 2, when $\theta_1 > \theta_c$, is given

[1] *D. Hondros and P. Debye,* Ann. Phys. ***32****, 466 (1910).*
[2] *H. Zahn,* Ann. Phys. ***49****, 907 (1916).*
[3] *H. Kogelnik, in* Guided Wave Optoelectronics, *(T. Tamir, Ed.), 2nd ed., Springer-Verlag, New York, 1990.*

by Eq. 6.12(7), which for $\mu_1 = \mu_2$, gives the decay coefficient in the x direction as

$$\alpha_x = \frac{\omega}{c} \varepsilon_{r2}^{1/2} \left[\frac{\varepsilon_1}{\varepsilon_2} \sin^2 \theta_1 - 1 \right]^{1/2} \tag{2}$$

The transverse field distribution in the lowest-order mode is sketched in Fig. 9.2*b*, and that for the next higher mode in Fig. 9.2*c*. The phase constant along the guide is

$$\beta = k_{1z} = k_1 \sin \theta_1 \tag{3}$$

Cutoff for the dielectric guide is considered the condition for which $\theta_1 = \theta_c$ at which point $\beta = k_2$. For steeper angles, $\theta_1 < \theta_c$, there is some energy transmission into the outer medium on each reflection, leading to leaky waves, as indicated in Fig. 9.2*d*.

For the interfering zigzag plane waves to form a mode, the phase lag after reflection from top and bottom and return to the top must be a multiple of 2π:

$$-2k_1 d \cos \theta_1 + 2\phi = m2\pi \tag{4}$$

where m is an integer and ϕ is the phase at reflection from medium 2. Using Sec. 6.11 we can find phase at reflection from ρ for TE and TM[4] waves, respectively, taking $\mu_1 = \mu_2$:

$$\phi_{TE} = 2 \tan^{-1} \left[\sqrt{\sin^2 \theta_1 - \varepsilon_2/\varepsilon_1} / \cos \theta_1 \right] \tag{5}$$

$$\phi_{TM} = 2 \tan^{-1} \left[\sqrt{\left(\frac{\varepsilon_1}{\varepsilon_2} \sin \theta_1 \right)^2 - \frac{\varepsilon_1}{\varepsilon_2}} \Big/ \cos \theta_1 \right] \tag{6}$$

The mode with $m = 0$ in (4) exists for arbitrarily small $k_1 d$ for both TE and TM modes, but for other values of m there is a minimum $k_1 d$ for cutoff (Prob 9.2d). For the $m = 0$ mode with $k_1 d$ small, α_x is also small so that fields extend well into the external region: i.e., the mode is only weakly guided (Prob. 9.2e).

The same physical principle of wave reflection at the interface applies to fibers and other dielectric guides of circular cross section, but the detailed development is more complicated. These will consequently be treated in Chapter 14 by a field analysis, together with a more detailed treatment of the planar guides.

9.3 Parallel-Plane Radial Transmission Lines

Linearly propagating waves between parallel planes were studied in Secs. 8.3–8.5 and a connection was made between the TEM wave and a transmission-line wave, where the two plates are the conductors of the line. Here we analyze radially propagating TEM waves between parallel conducting planes and introduce a transmission-line type of

[4] *For TM reflection coefficient defined in terms of an electric field component parallel to the interface, as in Sec. 6.11, there is an extra π in the phase at reflection. But this is a result of a reversal in spatial direction, compensated for on the next reflection.*

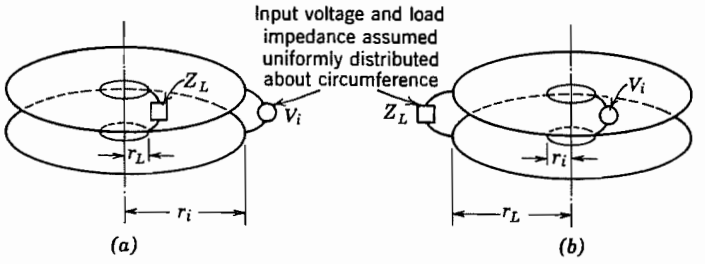

FIG. 9.3 (*a*) Radial transmission line with input at outer radius. (*b*) Radial transmission line with input at inner radius.

formalism to facilitate impedance-matching calculations (Figs. 9.3*a* and *b*). Higher-order modes are introduced in the following section. The wave under consideration has no field variations either circumferentially or axially. There are then field components E_z and H_ϕ only. The component E_z, having no variations in the z direction, corresponds to a total voltage $E_z d$ between plates. The component H_ϕ corresponds to a total radial current $2\pi r H_\phi$, outward in one plate and inward in the other. This wave is then analogous to an ordinary transmission-line wave and thus derives its name, radial transmission line.

For the simple wave described there are no radial field components, and analysis may be made by the nonuniform transmission-line theory of Sec. 5.17, allowing L and C to vary with radius. However, the wave solution for fields may also be obtained directly from the results of Sec. 7.20. Since there are no ϕ or z variations, ν and γ may be set equal to zero. Special linear combinations of Bessel functions have been defined particularly for this problem,[5] but for occasional solution of radial line problems, known forms of the Bessel functions are satisfactory. The form of Eq. 7.20(6) in the Hankel functions is particularly suitable since these can be shown to have the character of waves traveling radially inward or outward. Since $k_c = (\gamma^2 + k^2)^{1/2}$ by Eq. 8.2(19) and $\gamma = 0$ has been assumed, then $k_c = \omega\sqrt{\mu\varepsilon}$.

$$E_z = AH_0^{(1)}(kr) + BH_0^{(2)}(kr) \tag{1}$$

With ν and γ zero, the only remaining field component in Eqs. 8.9(1)–(4) is H_ϕ:

$$H_\phi = \frac{1}{j\omega\mu}\frac{\partial E_z}{\partial r} = \frac{j}{\eta}\left[AH_1^{(1)}(kr) + BH_1^{(2)}(kr)\right] \tag{2}$$

The $H_n^{(1)}$ terms are identified as the negatively traveling wave and the $H_n^{(2)}$ terms as the positively traveling wave because of the asymptotic forms that approach complex

[5] *N. Marcuvitz, in* Principles of Microwave Circuits *(C. G. Montgomery, R. H. Dicke, and E. M. Purcell, Eds.), Chap. 8, McGraw-Hill, New York, 1947.*

exponentials (Sec. 7.15). It is convenient to utilize the magnitudes and phases of these functions,

$$H_0^{(1)}(v) = J_0(v) + jN_0(v) = G_0(v)e^{j\theta(v)} \tag{3}$$

$$H_0^{(2)}(v) = J_0(v) - jN_0(v) = G_0(v)e^{-j\theta(v)} \tag{4}$$

$$jH_1^{(1)}(v) = -N_1(v) + jJ_1(v) = G_1(v)e^{j\psi(v)} \tag{5}$$

$$jH_1^{(2)}(v) = N_1(v) + jJ_1(v) = -G_1(v)e^{-j\psi(v)} \tag{6}$$

where

$$G_0(v) = [J_0^2(v) + N_0^2(v)]^{1/2}, \qquad \theta(v) = \tan^{-1}\left[\frac{N_0(v)}{J_0(v)}\right] \tag{7}$$

$$G_1(v) = [J_1^2(v) + N_1^2(v)]^{1/2}, \qquad \psi(v) = \tan^{-1}\left[\frac{J_1(v)}{-N_1(v)}\right] \tag{8}$$

Expressions (1) and (2) then become

$$E_z = G_0(kr)[Ae^{j\theta(kr)} + Be^{-j\theta(kr)}] \tag{9}$$

$$H_\phi = \frac{G_0(kr)}{Z_0(kr)}[Ae^{j\psi(kr)} - Be^{-j\psi(kr)}] \tag{10}$$

where

$$Z_0(kr) = \eta\frac{G_0(kr)}{G_1(kr)} \tag{11}$$

is a radially dependent characteristic wave impedance.

Evaluation of the constants A and B follows from specification of two field values at given radii. For example, given E_a at r_a and H_b at r_b, the fields at any radius r are

$$E_z = E_a\frac{G_0\cos(\theta - \psi_b)}{G_{0a}\cos(\theta_a - \psi_b)} + jZ_{0b}H_b\frac{G_0\sin(\theta - \theta_a)}{G_{0b}\cos(\theta_a - \psi_b)} \tag{12}$$

$$H_\phi = H_b\frac{G_1\cos(\psi - \theta_a)}{G_{1b}\cos(\theta_a - \psi_b)} + j\frac{E_aG_1\sin(\psi - \psi_b)}{Z_{0a}G_{1a}\cos(\theta_a - \psi_b)} \tag{13}$$

These are similar in form to the ordinary transmission-line equations except for the use of the special magnitudes and phases. A plot of these special radial line quantities versus kr is given in Fig. 9.3*c*. This is not very accurate for small values of kr, so the following approximations are then preferred:

$$G_0(v) \approx \frac{2}{\pi}\ln\left(\frac{\gamma v}{2}\right) \qquad \theta(v) \approx \tan^{-1}\left[\frac{2}{\pi}\ln\left(\frac{\gamma v}{2}\right)\right] \tag{14}$$

$$G_1(v) \approx \frac{2}{\pi v} \qquad \psi(v) \approx \tan^{-1}\left(\frac{1}{\pi v^2}\right) \tag{15}$$

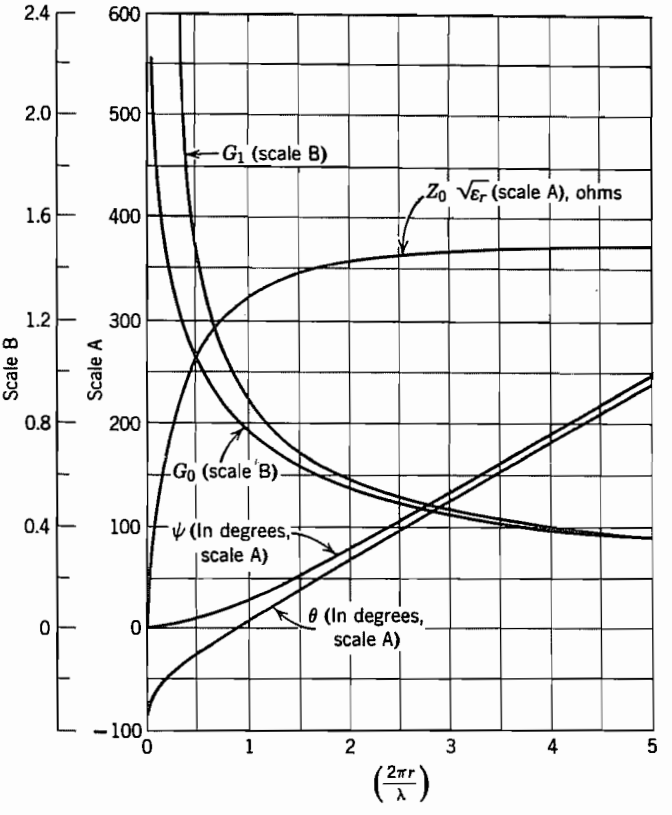

FIG. 9.3c Radial transmission-line quantities.

where $\gamma = 0.5772\ldots$. More accurate values can be calculated from the definitions (7) and (8) utilizing tables of J and N, although some tables give magnitude and phase of $H_n^{(1)}$ and $H_n^{(2)}$ directly.

Forms similar to (12) and (13) can be derived for two values of E_z specified at different radii or two values of H_ϕ. The most useful form, however, is that defining an input wave impedance $Z_i = E_{zi}/H_{\phi i}$ when load impedance $Z_L = E_{zL}/H_{\phi L}$ is given. This is

$$Z_i = Z_{0i}\left[\frac{Z_L \cos(\theta_i - \psi_L) + jZ_{0L}\sin(\theta_i - \theta_L)}{Z_{0L}\cos(\psi_i - \theta_L) + jZ_L \sin(\psi_i - \psi_L)}\right] \tag{16}$$

Special forms of this for output shorted ($Z_L = 0$) and open ($Z_L = \infty$) are especially simple and are analogous to the corresponding forms for uniform transmission lines.

All of the foregoing relationships are given in terms of fields or wave impedances.

Usually current, voltage, and total impedance are desired. The relations are

$$V = -E_z d, \qquad I = 2\pi r H_\phi \tag{17}$$

$$Z_{\text{total}} = \mp \frac{d}{2\pi r}\left(\frac{E_z}{H_\phi}\right) \tag{18}$$

The sign convention defines higher voltage in the upper plate and outward current in the upper plate as positive. The upper sign in (18) is for input radius less than that of the load, $r_i < r_L$, and the lower sign for the reverse, $r_i > r_L$, since in this case the convention for positive current would be the opposite of (17).

9.4 Circumferential Modes in Radial Lines: Sectoral Horns

Many higher-order modes can exist in the radial transmission lines studied in the last section. All those with z variations require a spacing between plates greater than a half-wavelength for radial propagation of energy. For smaller spacing, modes are possible with circumferential variations but no z variations. The field components may be written

$$E_z = A_\nu Z_\nu(kr) \sin \nu\phi \tag{1}$$

$$H_\phi = -\frac{j}{\eta} A_\nu Z'_\nu(kr) \sin \nu\phi \tag{2}$$

$$H_r = \frac{j\nu A_\nu}{k\eta r} Z_\nu(kr) \cos \nu\phi \tag{3}$$

In the foregoing equations, Z_ν denotes any solution of the ordinary νth order Bessel equation. For example, to stress the concept of radially propagating waves it may again be convenient to utilize Hankel functions:

$$Z_\nu(kr) = H_\nu^{(1)}(kr) + c_\nu H_\nu^{(2)}(kr) \tag{4}$$

These circumferential modes may be important as disturbing effects excited by asymmetries in radial lines intended for use with the symmetrical modes studied in the preceding section. In this case ν must be an integer since the wave must have the same value at $\phi = 0$ and $\phi = 2\pi$. Waves of the form (1) to (3) may also be supported in a wedge-shaped guide with conducting planes at $\phi = 0$ and $\phi = \phi_0$ as well as at $z =$

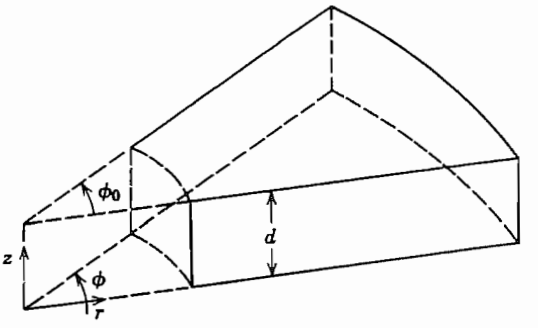

FIG. 9.4*a* Wedge-shaped guide or sectoral horn.

0, d (Fig. 9.4*a*). The latter case is important as a sectoral electromagnetic horn[6] used for radiation. In this case, since E_z must be zero at $\phi = 0, \phi_0$,

$$\nu = \frac{m\pi}{\phi_0} \tag{5}$$

The waves discussed here are interesting in one respect especially. If we think of the lowest-order mode ($m = 1$) propagating radially inward in the pie-shaped guide for Fig. 9.4*a*, it would be quite similar to the TE_{10} mode of the rectangular guide, although modified by the convergence of the sides. We would consequently expect a cutoff phenomenon at such a radius r_c that the width $r_c\phi_0$ becomes a half-wavelength. Similarly, for the lowest-order circumferential mode in the radial line of Figs. 9.3*a* and *b*, we would expect a cutoff at such a radius that circumference is one wavelength:

$$2\pi r_c = \lambda \text{ for radial line}, \qquad \phi_0 r_c = \frac{\lambda}{2} \text{ for sectoral horn} \tag{6}$$

A casual inspection of (1) to (3) would not reveal this cutoff since there is no sudden change of mathematical form as there was in the rectangular guide at cutoff. However, a more detailed study would reveal that there is a very effective cutoff phenomenon at about the radius predicted by (6) in that the reactive energy for given power transfer becomes very great for radii less than this. The radial field impedance for an inward traveling wave is

$$\left(\frac{E_z}{H_\phi}\right)_- = j\eta \frac{H_\nu^{(1)}(kr)}{H_\nu^{(1)'}(kr)} = R_\nu - jX_\nu \tag{7}$$

This impedance becomes predominantly reactive at a value $kr \approx \nu$, which is compatible with (6). Figure 9.4*b* shows real and imaginary parts of the wave impedances versus kr for $\nu = 9$.

[6] *W. L. Barrow and L. J. Chu,* Proc. IRE ***27****, 51 (1939).*

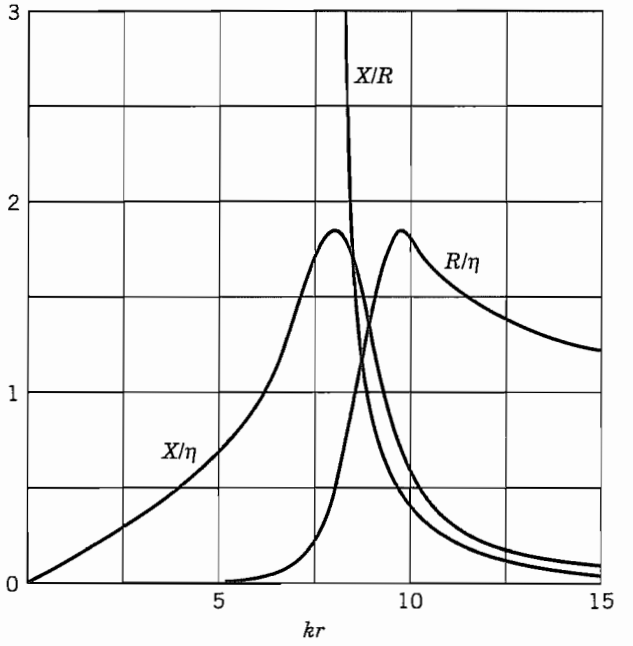

FIG. 9.4b Wave resistance and reactance for circumferential mode in radial line for $\nu = 9$.

9.5 DUALITY: PROPAGATION BETWEEN INCLINED PLANES

Given certain solutions of Maxwell's equations, we may obtain other useful ones by making use of the simple but important principle of duality. This principle follows from the symmetry of the field equations for charge-free regions:

$$\nabla \times \mathbf{E} = -j\omega\mu\mathbf{H} \tag{1}$$

$$\nabla \times \mathbf{H} = j\omega\varepsilon\mathbf{E} \tag{2}$$

It is evident that if $\mathbf{E}$ is replaced by $\mathbf{H}$, $\mathbf{H}$ by $-\mathbf{E}$, μ by ε, and ε by μ, the original equations are again obtained. It follows that if we are given any solution for such a dielectric, another may be obtained by interchanging components as stated. It may be difficult to supply appropriate boundary conditions for the new solution since the magnetic equivalent of the perfect conductor is not known at high frequencies, so the new solution is not always of practical importance.

One example in which the principle of duality may be utilized to save work in a practical problem is that of the principal mode in the wedge-shaped dielectric region between inclined plane conductors (Fig. 9.5). This mode has electric field E_ϕ and magnetic field H_z. If there are no variations with ϕ or z, it is evident that the field distri-

butions can be obtained from those of the radial transmission-line mode (Sec. 9.3) through the foregoing principle of duality. Replacing **E** by **H**, **H** by $-\mathbf{E}$, μ by ε, and ε by μ in Eqs. 9.3(1) and 9.3(2),

$$H_z = AH_0^{(1)}(kr) + BH_0^{(2)}(kr) \tag{3}$$

$$E_\phi = -j\sqrt{\frac{\mu}{\varepsilon}}\,[AH_1^{(1)}(kr) + BH_1^{(2)}(kr)] \tag{4}$$

The real advantage is that all the derived expressions 9.3(9)–(16) may be used without rederivation, as may the curves of Fig. 9.3*c*, with the interchange of quantities as above. Admittance should be read in place of impedance, and the numerical scale of $Z_0\sqrt{\varepsilon_r}$ in ohms (Fig. 9.3*c*) should be divided by $(377)^2$ to give the characteristic admittance $Y_0/\sqrt{\varepsilon_r}$ in siemens. Total admittance is obtained from the field admittance by

$$Y_{\text{total}} = \mp \frac{l}{r\phi_0}\left[\frac{H_z}{E_\phi}\right] \tag{5}$$

where the upper sign is for $r_i < r_L$, and the lower for $r_i > r_L$.

Example 9.5
Use of Inclined Planes for Impedance Matching

One application of the inclined-plane transmission line might be in impedance matching between parallel-plate transmission lines of different spacings, d_1 and d_2 (Fig. 9.5). It is known from practical experience that such transitions, if gradual enough, supply a good impedance match over a wide band of frequencies (unlike schemes studied in Prob. 5.7*c*, which depend upon quarter-wavelengths of line). It is seen from Fig. 9.3*c* that for both kr_i and kr_L large (say, greater than 5) the characteristic admittance Y_0 is nearly $1/\eta$ and θ and ψ are nearly equal (i.e., $\theta_i \approx \psi_i$, $\theta_L \approx \psi_L$). If the parallel-plane

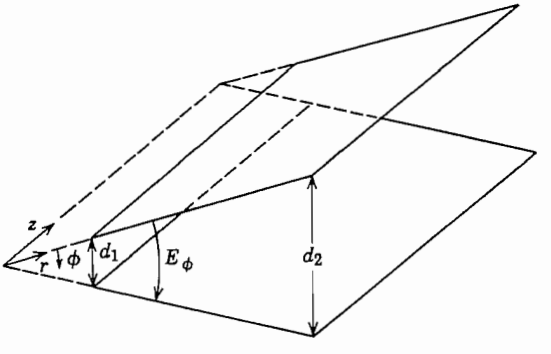

Fig. 9.5 Inclined-plane guide.

line to the right is matched, its characteristic wave admittance is that of a plane wave, $1/\eta$. Equation 9.3(16) then shows that with the above approximations the input wave admittance is also approximately $1/\eta$, so that the parallel-plane line to the left is also nearly matched. This gives some quantitative support to the matching phenomenon mentioned.

9.6 Waves Guided by Conical Systems

The problem of waves guided by conical systems (Fig. 9.6) is important to a basic understanding of waves along dipole antennas and in certain classes of cavity resonators. In particular, one very important wave propagates along the cones with the velocity of light, has no field components in the radial direction, and so is analogous to the transmission-line wave on cylindrical systems. This basic wave is symmetric about the axis of the guiding cones, so that if the two curl relations of Maxwell's equations are written in spherical coordinates with all ϕ variation eliminated, it is seen that there is one independent set containing E_θ, H_ϕ, and E_r only:

$$\frac{1}{r}\frac{\partial(rE_\theta)}{\partial r} - \frac{1}{r}\frac{\partial E_r}{\partial \theta} + j\omega\mu H_\phi = 0 \tag{1}$$

$$\frac{1}{r\sin\theta}\left[\frac{\partial}{\partial\theta}(\sin\theta H_\phi)\right] - j\omega\varepsilon E_r = 0 \tag{2}$$

$$-\frac{1}{r}\frac{\partial(rH_\phi)}{\partial r} - j\omega\varepsilon E_\theta = 0 \tag{3}$$

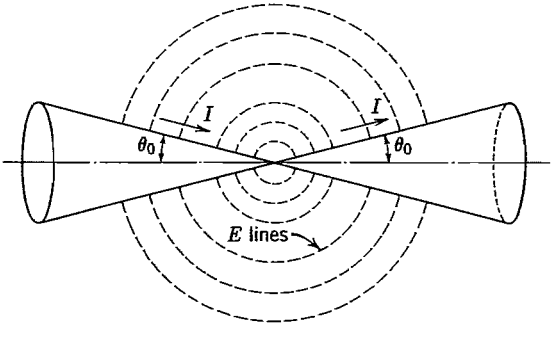

Fig. 9.6 Biconical guide.

It can be checked by substitution that the following solution does satisfy the three equations:

$$E_r = 0 \tag{4}$$

$$rE_\theta = \frac{\eta}{\sin\theta}\left[Ae^{-jkr} + Be^{jkr}\right] \tag{5}$$

$$rH_\phi = \frac{1}{\sin\theta}\left[Ae^{-jkr} - Be^{jkr}\right] \tag{6}$$

These equations show the now-familiar propagation behavior, the first term representing a wave traveling radially outward with the velocity of light in the dielectric material surrounding the cones, the second term representing a radially inward traveling wave of the same velocity. The ratio of electric to magnetic field E_θ/H_ϕ is given by η for the positively traveling wave and by $-\eta$ for the negatively traveling wave. There is no field component in the radial direction, which is the direction of propagation.

The above wave looks much like the ordinary transmission-line waves of uniform cylindrical systems. This resemblance is stressed if we note that the E_θ corresponds to a voltage difference between the two cones,

$$\begin{aligned} V &= -\int_{\theta_0}^{\pi-\theta_0} E_\theta r\, d\theta = -\eta \int_{\theta_0}^{\pi-\theta_0} \frac{d\theta}{\sin\theta}\left[Ae^{-jkr} + Be^{jkr}\right] \\ &= 2\eta \ln\cot\frac{\theta_0}{2}\left[Ae^{-jkr} + Be^{jkr}\right] \end{aligned} \tag{7}$$

where the case treated is that of equal-angle cones (Fig. 9.6). This is a voltage which is independent of r, except through the propagation term, $e^{\pm jkr}$. Similarly the azimuthal magnetic field corresponds to a current flow in the cones at $\theta = \theta_0$:

$$\begin{aligned} I &= 2\pi r H_\phi \sin\theta_0 \\ &= 2\pi\left[Ae^{-jkr} - Be^{jkr}\right] \end{aligned} \tag{8}$$

This current is also independent of radius, except through the propagation term. A study of the sign relations shows that it is in opposite radial directions in the two cones at any given radius.

The ratio of voltage to current in a single outward-traveling wave, a quantity which we call characteristic impedance in an ordinary transmission line, is obtained from (7) and (8) with $B = 0$:

$$Z_0 = \frac{\eta \ln\cot\theta_0/2}{\pi} \tag{9}$$

For a negatively traveling wave, the ratio of voltage to current is the negative of this quantity. This value of impedance is a constant, independent of radius, unlike those ratios defined for a parallel-plane radial transmission line in Sec. 9.3. We can also see this starting from the familiar concept of Z_0 as $\sqrt{L/C}$, since inductance and capacitance

between cones per unit radial length are independent of radius. This comes about since surface area increases proportionally to radius, and distance separating the cones along the path of the electric field also increases proportionally to radius.

So far as this wave is concerned, the system arising from two ideal coaxial conical conductors can be considered a uniform transmission line. All the familiar formulas for input impedances and voltage and current along the line hold directly, with Z_0 given by (9) and phase constant corresponding to velocity of light in the dielectric:

$$\beta = \frac{2\pi}{\lambda} = \omega\sqrt{\mu\varepsilon} \tag{10}$$

If the conducting cones have resistance, there is a departure from uniformity due to this resistance term, but this is usually not serious in any practical cases where such conical systems are used.

Of course, a large number of higher-order waves may exist in this conical system and in similar systems. These will in general have field components in the radial direction and will not propagate at the velocity of light. We shall consider such general wave types for spherical coordinates in Sec. 10.7.

9.7 Ridge Waveguide

Of the miscellaneous shapes of cylindrical guides that have been utilized, one rather important one is the ridge waveguide, which has a central ridge added to either the top or bottom, or both, of a rectangular section as in Fig. 9.7*a*. It is interesting from an electromagnetic point of view since the cutoff frequency is lowered because of the capacitive effect at the center, and could in principle be made as low as desired by decreasing the gap width g sufficiently. Of course, the effective impedance of the guide also decreases as g is made smaller. One of the important applications is as a nonuniform transmission system for matching purposes obtained by varying the depth of ridge along the guide, similar to the approach described in Sec. 9.5.

The calculation of cutoff frequency, which is a very important parameter for any shape of guide, also illustrates an interesting approach that may be applied to many guide shapes which cannot be solved exactly. At cutoff, there is no variation in the z direction ($\gamma = 0$), so one may think of this as a resonant condition for waves propagating only transversely in the given cross section, according to the desired mode. For example, the TE_{10} wave in a rectangular guide has a cutoff frequency equal to the resonant frequency for a plane wave propagating only in the x direction across the guide, thus corresponding to a half-wavelength in the x direction. A very approximate calculation of cutoff frequency for the ridge guide might then be made as in Fig. 9.7*a* by considering the gap a capacitance and the side sections one-turn solenoidal inductances, and writing the condition for resonance:

$$f_c = \frac{1}{2\pi}\left(C_B \frac{L_A}{2}\right)^{-1/2} = \frac{1}{2\pi}\left(\frac{2d\varepsilon}{g}\right)^{-1/2}\left(\frac{\mu lh}{2}\right)^{-1/2} = \frac{1}{2\pi}\left(\frac{g}{\mu\varepsilon lhd}\right)^{1/2} \tag{1}$$

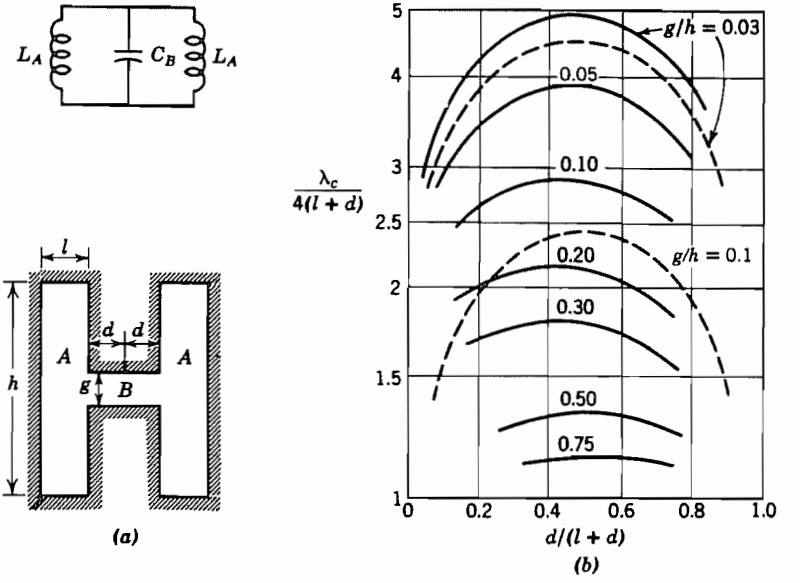

FIG. 9.7 (*a*) Cross section of ridge waveguide and approximate equivalent circuit for cutoff calculation. (*b*) Curves giving cutoff wavelength for a ridge waveguide as in (*a*). Solid curves: data from Cohn.[7] Dashed curves from Eq. (1).

A better equivalent circuit for calculation of the transverse resonance is one in which the two sections A and B are considered parallel-plane transmission lines with a discontinuity capacitance C_d placed at the junction between them. (This junction effect will be discussed in Chapter 11.) Curves of cutoff frequency and a total impedance for the guide have been calculated in this manner by Cohn.[7] Some results are shown in Fig. 9.7*b* with comparisons of results from the lumped element approximation (1). As might be expected, agreement is better for the smaller gaps. The technique of finding cutoff by calculating transverse resonance frequencies—often by numerical means[8]—is valuable for a variety of irregularly shaped guides.

The ridge guide illustrates that guides other than two-conductor transmission lines can be appreciably smaller than the half-wavelength measure found for the rectangular and circular guides if the boundaries concentrate energy appropriately. However, the boundary irregularities generally decrease power-handling capacity.

[7] *S. B. Cohn*, Proc. IRE ***35***, *783–788 (1947).*

[8] *See, for example, R. Bulley*, IEEE Trans. Microwave Theory Techniques ***MTT-18***, *1022 (1970).*

9.8 The Idealized Helix and Other Slow-Wave Structures

A wire wound in the form of a helix (Fig. 9.8*a*) makes a type of guide that has been found useful for antennas[9] and as slow-wave structures in traveling-wave tubes.[10] It is interesting as an example of a general class of structures that possess waves with a phase velocity along the axis much less than the velocity of light, as contrasted with most of the waves so far studied, which have phase velocities greater than the velocity of light. A rough picture suggests that the wave might follow the wire with about the velocity of light, so that its rate of progress along the axis would correspond to a phase velocity

$$v_p \approx c \sin \psi \tag{1}$$

where ψ is the pitch angle. It is rather surprising that this represents a good approximation over a wide range of parameters. It is also interesting to find that a useful analysis can be made by considering an idealization of the actual helix.

The idealization commonly analyzed,[10] referred to as the helical sheet, is a cylindrical surface in which the component of electric field along the direction of ψ is assumed to be zero at all points of the sheet (Fig. 9.8*b*). Moreover, the component of electric field lying in the cylindrical surface normal to the direction of ψ is assumed to be continuous through the surface, as is the component of magnetic field along ψ (the latter because there is to be no current flow normal to the direction of ψ). Since the idealization takes

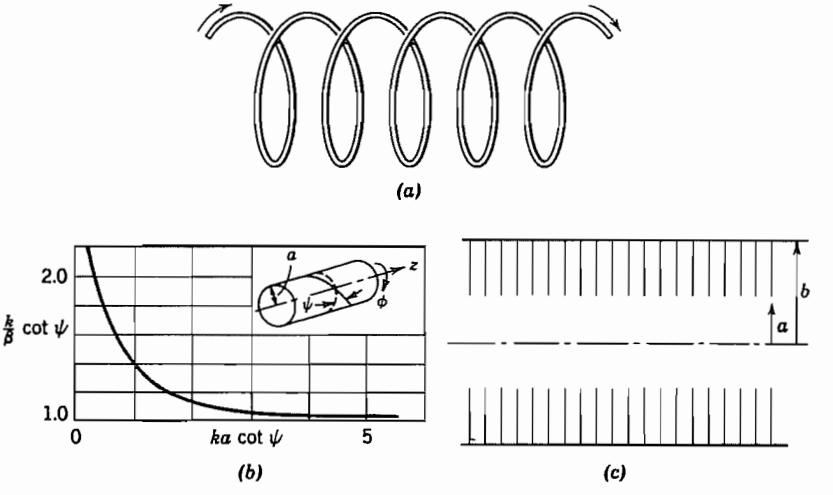

Fig. 9.8 (*a*) Wire helix. (*b*) Idealized conducting sheet and curve giving propagation constant.[10] (*c*) Section of disk-loaded waveguide.

[9] *J. D. Kraus,* Antennas, *2nd ed., Chap. 7, McGraw-Hill, New York, 1988.*

[10] *J. R. Pierce,* Traveling-Wave Tubes, *Chap. III and Appendix II, Van Nostrand, Princeton, NJ, 1950.*

these conditions to be the same over all the sheet, it would be expected to give best results for fine-wire helices of small pitch angle or for multifilar helices with fine wires close together.

To find the propagation constant, we set up the general solutions inside and outside the helical sheet and match them at the boundary according to continuity conditions stated above. The wave that satisfies the boundary conditions is a hybrid mode containing both TE and TM components. We assume an unattenuated wave so that $\gamma = j\beta$. Then the separation constant in the general solutions [Eqs. 7.20(5)] is $k_c^2 = k^2 + \gamma^2 = k^2 - \beta^2$. Since $k = \omega/c$ and $\beta = \omega/v_p$, $\beta > k$ for waves with phase velocities below the speed of light. Therefore, $k_c^2 < 0$ and $k_c = j\tau$, where τ is a real quantity. Assuming axial symmetry and that the fields must be finite on the axis and zero at infinite radius, the general solutions can be expressed in terms of modified Bessel functions [Eqs. 7.14(16) and (17)]. The z variation $e^{-j\beta z}$ is understood in all of the following:

$$r < a \qquad\qquad r > a$$

$$E_{z1} = A_1 I_0(\tau r) \qquad E_{z2} = A_2 K_0(\tau r) \tag{2}$$

$$E_{r1} = \frac{j\beta}{\tau} A_1 I_1(\tau r) \qquad E_{r2} = -\frac{j\beta}{\tau} A_2 K_1(\tau r) \tag{3}$$

$$H_{\phi 1} = \frac{j\omega\varepsilon}{\tau} A_1 I_1(\tau r) \qquad H_{\phi 2} = -\frac{j\omega\varepsilon}{\tau} A_2 K_1(\tau r) \tag{4}$$

$$H_{z1} = B_1 I_0(\tau r) \qquad H_{z2} = B_2 K_0(\tau r) \tag{5}$$

$$H_{r1} = \frac{j\beta}{\tau} B_1 I_1(\tau r) \qquad H_{r2} = -\frac{j\beta}{\tau} B_2 K_1(\tau r) \tag{6}$$

$$E_{\phi 1} = -\frac{j\omega\mu}{\tau} B_1 I_1(\tau r) \qquad E_{\phi 2} = \frac{j\omega\mu}{\tau} B_2 K_1(\tau r) \tag{7}$$

The idealized boundary conditions first described are

$$E_{z1} \sin\psi + E_{\phi 1} \cos\psi = 0 \tag{8}$$

$$E_{z2} \sin\psi + E_{\phi 2} \cos\psi = 0 \tag{9}$$

$$E_{z1} \cos\psi - E_{\phi 1} \sin\psi = E_{z2} \cos\psi - E_{\phi 2} \sin\psi \tag{10}$$

$$H_{z1} \sin\psi + H_{\phi 1} \cos\psi = H_{z2} \sin\psi + H_{\phi 2} \cos\psi \tag{11}$$

The fields (2)–(7) are substituted in (8)–(11). A nonvanishing solution for the field amplitude requires that the determinant of the coefficients be zero, which leads to

$$(\tau a)^2 \frac{I_0(\tau a) K_0(\tau a)}{I_1(\tau a) K_1(\tau a)} = (ka \cot\psi)^2 \tag{12}$$

A solution of this taken from Pierce[10] is shown in Fig. 9.8*b*. It is seen that for $ka \cot\psi > 4$, the approximation (1) gives good results.

Some general comments about slow-wave structures are in order. If it is desired to produce a wave with an electric field along the axis, propagating with a phase velocity less than that of light (as in a traveling-wave tube where the phase velocity should be approximately equal to the beam velocity for efficient interaction with the electrons), then, as discussed above, $k_c^2 < 0$:

$$\tau^2 = -k_c^2 = \beta^2 - k^2 \tag{13}$$

$$\tau = \beta\left(1 - \frac{v_p^2}{c^2}\right)^{1/2} \tag{14}$$

It is consequently necessary in a cylindrically symmetric system that the Bessel function solutions (Sec. 7.20) have imaginary arguments, and they may therefore be written as modified Bessel functions. For a TM wave,

$$E_z = AI_0(\tau r) \tag{15}$$

$$H_\phi = \frac{\omega\varepsilon}{\beta} E_r = \frac{j\omega\varepsilon}{\tau} AI_1(\tau r) \tag{16}$$

Example 9.8

CYLINDRICAL REACTANCE WALL TO PRODUCE SLOW WAVES

If we ask about the boundary conditions that might be supplied at a cylindrical surface $r = a$ to support slow waves, we see that, if uniform, it should be of the nature of a reactive sheet with

$$jX = -\left.\frac{E_z}{H_\phi}\right|_{r=a} = j\eta\frac{\tau}{k}\frac{I_0(\tau a)}{I_1(\tau a)} \tag{17}$$

The helical sheet studied earlier may be considered as supplying this required reactance through the interaction with the TE waves and external fields caused by the helical cuts. The short-circuited sections of radial lines of a disk-loaded waveguide (Fig. 9.8*c*) may also be considered as supplying an approximation to the above required uniform reactance at $r = a$, and will therefore support a slow wave also. The approximate reactance supplied by this structure is

$$X = \eta\left[\frac{J_0(ka)N_0(kb) - J_0(kb)N_0(ka)}{J_1(ka)N_0(kb) - J_0(kb)N_1(ka)}\right] \tag{18}$$

Note that if $(v_p/c)^2 \ll 1$, τ is substantially equal to β. By the nature of the I_0 functions (Fig. 7.14*c*), the field on the axis of such slow-wave structures is much less than that on the boundary when βa is large. This is of course undesirable when it is the field on the axis that is to act on electrons, as in a traveling-wave tube. Of course, the presence of electron space charge will modify the forms of solution somewhat.

9.9 SURFACE GUIDING

The result of Sec. 9.8 suggests a localization of fields near a surface that possesses a reactive surface impedance. This concept appeared there in an interior region, but may be useful when the fields are in the external region also. Because of the surface-guiding principle, the energy is maintained near the surface so that it is not radiated or coupled seriously to nearby objects. Thus the external region corresponding to Fig. 9.8*c* would be as shown in Fig. 9.9*a*. The proper solutions for the external cylindrical region for a TM wave are the same as Eqs. 9.8(2)–(4) for $r > a$. For E_z and H_ϕ, with $e^{-j\beta z}$ understood,

$$E_z = AK_0(\tau r) \tag{1}$$

$$H_\phi = -\frac{j\omega\varepsilon}{\tau} AK_1(\tau r) \tag{2}$$

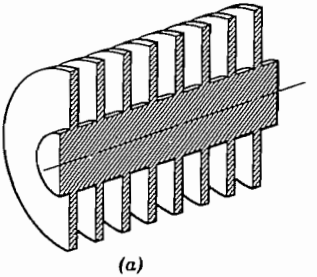

(a)

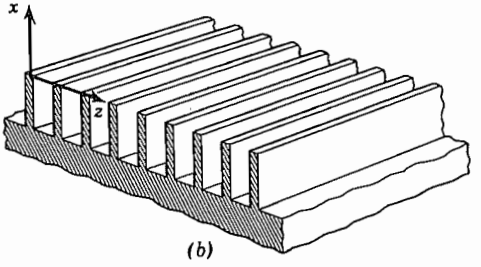

(b)

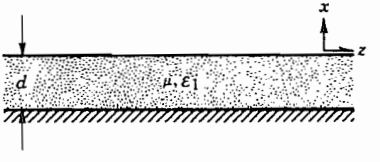

(c)

FIG. 9.9 (*a*) Rod with periodic radius variations capable of propagating a slow wave. (*b*) Planar equivalent of (*a*). (*c*) Dielectric-coated conducting surface.

The field reactance at $r = a$ necessary to support such a wave is then

$$jX = \left.\frac{E_z}{H_\phi}\right|_{r=a} = j\eta \frac{\tau}{k} \frac{K_0(\tau r)}{K_1(\tau r)} \tag{3}$$

Equation (3) again represents a positive, or inductive, reactance as did Eq. 9.8(17), and the solutions (1) and (2) die off for large r. Phase velocity is less than the velocity of light in the external dielectric in order to maintain τ real, as in Eq. 9.8(13):

$$\tau^2 = \beta^2 - k^2 \tag{4}$$

Example 9.9a

SURFACE GUIDING BY A REACTANCE SHEET

The above concept is perhaps more easily visualized for a plane sheet, as pictured in Fig. 9.9*b*. Substitution in Eqs. 8.2(13)–(16) easily verifies that the following are solutions of Maxwell's equations, using the definition (4), again with $e^{-j\beta z}$ understood:

$$E_z = Ce^{-\tau x} \tag{5}$$

$$H_y = -\frac{j\omega\varepsilon C}{\tau} e^{-\tau x} \tag{6}$$

$$E_x = -\frac{j\beta C}{\tau} e^{-\tau x} \tag{7}$$

A surface wave impedance defined for this example is then

$$jX = \left.\frac{E_z}{H_y}\right|_{x=0} = \frac{j\tau}{\omega\varepsilon} \tag{8}$$

Again we see that the impedance sheet should be inductive for surface guiding of this TM wave (but see Prob. 9.9a), and that the value of β must be greater than k if the wave is to die away with increasing x. Therefore, phase velocity is less than the velocity of light in the dielectric. The spaces between the conducting fins may be considered to be shorted parallel-plane transmission lines and the field impedance at the ends of the fins can be found from Sec. 8.3 as

$$\frac{E_z}{H_y} = j\eta \tan kd$$

where d is the height of the fins. It is clear that if $kd < \pi/2$, the surface appears as an inductive reactance.

Example 9.9b
SURFACE GUIDING BY A DIELECTRIC COATING

Another important way of obtaining a surface impedance sheet is by coating a conductor with a thin layer of dielectric, as illustrated in Fig. 9.9*c*. The following TM solutions for region 1 can be verified by substitution in Eqs. 8.2(13)–(16). The conductor is assumed perfect and the argument of the sine is selected to make E_z zero at the conductor surface, $x = -d$:

$$E_z = D \sin k_x(x + d) \tag{9}$$

$$H_y = -\frac{j\omega\varepsilon_1 D}{k_x} \cos k_x(x + d) \tag{10}$$

$$E_x = -\frac{j\beta D}{k_x} \cos k_x(x + d) \tag{11}$$

$$k_x^2 = k_1^2 - \beta^2 \tag{12}$$

From (9) and (10) a field impedance at $x = 0$ can be found as follows:

$$jX = \left.\frac{E_z}{H_y}\right|_{x=0} = \frac{jk_x}{\omega\varepsilon_1} \tan k_x d \tag{13}$$

This is inductive as required for guiding TM waves and, if equated to (8), will define the β of the desired surface wave. For small thickness, $k_x d \ll 1$, (13) becomes

$$jX \approx \frac{jk_x^2 d}{\omega\varepsilon_1} \tag{14}$$

Using (4), (8), (12), and (14), we can show that the phase velocity is less than the velocity of light in the external dielectric and greater than that in the coating.

The principle is also applicable to lossy dielectrics and/or conductors, for which a finite but relatively small attenuation in the z direction is obtained. Zenneck[11] and Sommerfeld[12] provided the early classical analyses of this phenomenon; Goubau[13] illustrated its usefulness as a practical wave-guiding means by using either thin dielectric coatings or corrugations on round wires; a thorough treatment is given by Collin.[14] Surface guiding and dielectric wave guiding are closely related phenomena since one boundary is a dielectric interface as treated in Sec. 9.2. The relationship will become clearer with the field analysis of dielectric guides in Chapter 14.

---

[11] *J. Zenneck,* Ann. Phys. ***23****, 846 (1907).*

[12] *A. Sommerfeld,* Ann. Phys. Chem. ***67****, 233 (1899). Described in J. A. Stratton,* Electromagnetic Theory, *p. 527, McGraw-Hill, New York, 1946.*

[13] *G. Goubau,* Proc. IRE ***39****, 619 (1951);* J. Appl. Phys. ***21****, 1119 (1950).*

[14] *R. E. Collin,* Field Theory of Guided Waves, *2nd ed., Chap. 11, IEEE Press, Piscataway, NJ, 1991.*

9.10 Periodic Structures and Spatial Harmonics

The corrugated surfaces used as illustrations of reactance walls in the two preceding sections are special examples of periodic systems if the spacing between corrugations is uniform. Periodic systems have interesting properties and important applications and so will be examined more carefully in this section. We recognize that the treatment as a smooth reactance wall, used in Secs. 9.8 and 9.9, is only an approximation since the grooves will cause field disturbances not accounted for by this "smoothed out" approximation.

Let us begin by consideration of a specific example, the parallel-plane transmission line with periodic troughs in one plate, as illustrated in Fig. 9.10*a*. If the troughs are relatively narrow, they act to waves with z-directed currents in the bottom plate as shorted transmission lines in series with the conductor. These lines produce values of E_z and H_y at $x = 0$, which are essentially constant over the gap width w. Thus the boundary condition for E_z at $x = 0$ is as shown in Fig. 9.10*b*, a phase shift of $\beta_0 d$ being allowed over each period since we will stress propagating waves. The square waves shown neglect higher-order fringing fields at the corners, but are better approximations than the complete smoothing out of the effect (as in Sec. 9.9) and are sufficient to illustrate the basic properties of periodic structures.

To fulfill the boundary condition at $x = 0$, we might expect to add solutions of Maxwell's equations just as we added solutions of Laplace's equation in Chapter 7 to satisfy boundary conditions not satisfied by a single solution.

For the present problem let us take $\partial/\partial y = 0$ and consider waves with E_x, E_z, and H_y only. Thus a sum of solutions satisfying Maxwell's equations and the boundary condition of $E_z = 0$ at $x = a$ may be written by adding waves of the TM form, the TEM component being included if the sum includes $n = 0$:

$$E_z(x, z) = \sum_{n=-\infty}^{\infty} A_n \sin K_n(a - x)e^{-j\beta_n z} \tag{1}$$

$$E_x(x, z) = \sum_{n=-\infty}^{\infty} \frac{j\beta_n}{K_n} A_n \cos K_n(a - x)e^{-j\beta_n z} \tag{2}$$

$$H_y(x, z) = \sum_{n=-\infty}^{\infty} \frac{j\omega\varepsilon}{K_n} A_n \cos K_n(a - x)e^{-j\beta_n z} \tag{3}$$

where

$$K_n^2 = \omega^2\mu\varepsilon - \beta_n^2 = k^2 - \beta_n^2 \tag{4}$$

The boundary condition illustrated by Fig. 9.10*b* is a periodic function of z if the phase factor is taken out separately. If we expand the resulting periodic function in the complex form of the Fourier series (Prob. 7.11e), we may write for the boundary condition

$$E_z(0, z) = e^{-j\beta_0 z} \sum_{n=-\infty}^{\infty} C_n e^{-(j2\pi nz/d)} \tag{5}$$

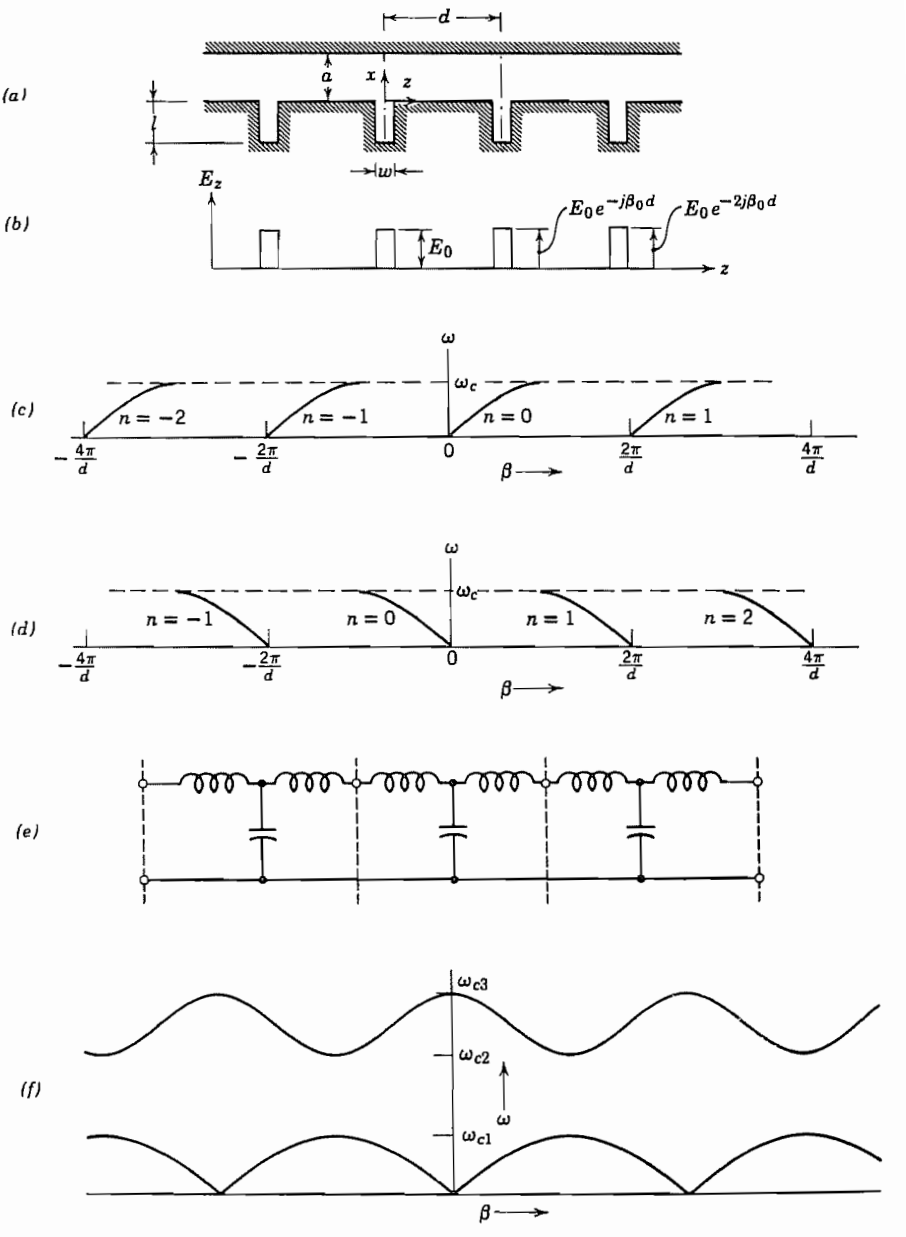

FIG. 9.10 (*a*) Parallel-plane transmission line with periodic short-circuited troughs. (*b*) Idealized variations of E_z along the lower plate in the structure of (*a*). (*c*) ω–β relation for spatial harmonics of wave with fundamental traveling in $+z$ direction. (*d*) ω–β relation for spatial harmonics of wave with fundamental traveling in $-z$ direction. (*e*) Low-frequency equivalent circuit for fundamental spatial harmonic of structure in (*a*). (*f*) Composite ω–β diagram including passband at higher frequency.

where

$$C_n = \frac{1}{d}\int_{-d/2}^{d/2} E_z(0, z)e^{j\beta_0 z}e^{+j(2\pi nz/d)}\,dz = \frac{1}{d}\int_{-w/2}^{w/2} E_0 e^{+j(2\pi nz/d)}\,dz$$

$$= \frac{E_0}{\pi n}\sin\left(\frac{n\pi w}{d}\right) \tag{6}$$

By comparing (5) with (1) evaluated at $x = 0$, we can now identify A_n and β_n:

$$A_n = \frac{C_n}{\sin K_n a} = \frac{E_0}{\pi n}\frac{\sin(n\pi w/d)}{\sin K_n a} \tag{7}$$

$$\beta_n = \beta_0 + \frac{2\pi n}{d} \tag{8}$$

A wave solution is thus determined for this problem with the approximations described.

We wish first to stress the different role of the TM solutions in this problem compared with that considered previously. In earlier sections TM solutions have been considered as "modes" with the inference that each may be excited independently. Here they are coupled by the periodic boundary condition and must exist in the proper relationship to each other to satisfy this boundary condition. In this capacity they are known as "spatial harmonics," a natural extension of the harmonic character of the Fourier series to the periodic system in space. We note especially from (8) that determination of β for any spatial harmonic automatically determines the value of all others. Thus the ω–β diagram (Sec. 5.12) is periodic in β with repetition at intervals of $2\pi/d$ as illustrated in Figs. 9.10*c* and *d*.

Determination of the shape of one period of this plot (say β_0) requires study of the boundary conditions on two field components. We have already considered E_z and now choose H_y as the second component for this example. If the solution for the troughs is well approximated by the shorted-transmission-line behavior, the value of H_y at $x = 0$, $z = 0$ for the shorted lines is given by

$$H_y = \frac{-jE_0}{\eta}\cot kl$$

Thus one might equate this to (3) evaluated at $x = 0$, and A_n substituted from (7):

$$-\frac{j}{\eta}\cot kl = \sum_{n=-\infty}^{\infty}\frac{j\omega\varepsilon}{\pi n K_n}\sin\frac{\pi nw}{d}\cot K_n a \tag{9}$$

This with (4) and (8) determines β_0 in principle, although the general solution may be difficult.

For the special case of $\beta_0 d \ll 1$, lumped-element approximations may be used. The fundamental harmonic solution of the corresponding low-pass filter then gives the characteristics of the fundamental, and from that, the values of β for other spatial harmonics. The filter corresponding to the line used in the above example is shown in Fig. 9.10*e*. The shunt capacitance and a part of the series inductance represent the fields in the parallel-plate section between grooves, and the shorted-transmission-line grooves con-

tribute an additional series inductance. The capacitors in Fig. 9.10*e* each have the value $C = \varepsilon(d - w)/a$ for a unit length in the y direction. The inductance from the section between grooves is $L_1 = \mu a(d - w)$ and that from the shorted grooves is $L_2 = (\eta w/\omega)$ tan kl (assuming $kl < \pi/2$). Each inductor in Fig. 9.10*e* has the value $L = (L_1 + L_2)/2$.

Although illustrated for a particular example to provide concreteness, the periodic character of the ω–β diagram and the relation (8) for phase constant of a spatial harmonic apply to any structure of period d. Other important properties are as follows:

1. The group velocities of all spatial harmonics of a given wave are equal. This would be expected so that the wave would stay together, but may be noted either from the ω–β diagrams or by differentiating (8):

$$\frac{1}{v_{gn}} = \frac{d\beta_n}{d\omega} = \frac{d\beta_0}{d\omega}$$

2. Of the infinite number of spatial harmonics, half are backward waves (Sec. 5.16) with phase and group velocities in the opposite directions. Thus the $n = 0, 1, 2,$ and so on of Fig. 9.10*c* are forward waves, whereas $n = -1, -2,$ and so on are backward waves, as is seen by comparing the signs of ω/β and $d\omega/d\beta$ for the various portions of the figure. If the phase velocity of the fundamental spatial harmonic is negative, the harmonics are as shown in Fig. 9.10*d*. Here the $n = 0, -1, -2,$ and so on have both phase and group velocities in the negative direction and are not backward waves, whereas the $n = 1, 2,$ and so on are backward waves with positive phase velocities and negative group velocities. The structure of Fig. 9.10*a* has a fundamental forward wave, but other periodic structures may have fundamental backward waves.
3. The field distribution at any plane $z = md$ (m an integer) is the same as at $z = 0$ except for multiplication by the phase $e^{-j\beta_0 md}$. This important property is related to Floquet's theorem,[15] and is often taken as the fundamental starting point for the study of periodic systems. For the particular example used in this section, (1) and (8) yield

$$\begin{aligned} E_z(x, md) &= \sum_{n=-\infty}^{\infty} A_n \sin K_n(a - x) e^{-j\beta_0 md} e^{-j2\pi mn} \\ &= e^{-j\beta_0 md} \sum_{n=-\infty}^{\infty} A_n \sin K_n(a - x) = e^{-j\beta_0 md} E_z(x, 0) \end{aligned} \tag{10}$$

and similarly for the other field components.

4. The wave is cut off where group velocity becomes zero, shown as ω_c in Figs. 9.10*c* and *d*. Above this frequency there is a region of reactive attenuation, typical of filters in the attenuating region. As frequency is increased, however, other pass bands will be found with propagating waves, as illustrated in Fig. 9.10*f*. Each of

[15] *R. E. Collin,* Field Theory of Guided Waves, *2nd ed., Sec. 9.1, IEEE Press, Piscataway, NJ, 1991.*

these waves has spatial harmonics, just as the low-pass wave studied. The Pierce coupled-mode theory[16] is especially powerful in giving a picture of the entire ω–β diagram in a structure with relatively small periodic perturbations if the phase constants of the unperturbed system are known.

PROBLEMS

9.2a For a dielectric slab guide with $\mu_1 = \mu_2$, plot the complement of the critical angle of Fig. 9.2*a*, $\psi = \pi/2 - \theta_c$, as a function of $\varepsilon_2/\varepsilon_1$. Many dielectric guides have small differences between the two permittivities, ε_2 and $\varepsilon_1(1 - \Delta)$, where $\Delta \ll 1$. For these, show that $\psi \approx \sqrt{\Delta}$.

9.2b Demonstrate that when $\theta = \theta_c$ (defined as cutoff for the dielectric slab guides), there is no decay in medium 2 (outside of slab) and propagation is at the velocity of light in medium 2. Show that when θ approaches $\pi/2$ (grazing incidence at the boundary), phase velocity approaches the velocity of light in medium 1.

9.2c Using the definition of cutoff given in Prob. 9.2b, show that the x component of k_1 at cutoff is $k_{1x} = (k_1^2 - k_2^2)^{1/2}$. Calculate the lowest cutoff frequencies (other than zero) for TM modes with even and odd symmetry of E_z across the slab and similarly for TE modes with even and odd symmetries of H_z with $d = 1$ mm, $\varepsilon_1 = 4.08\varepsilon_0$, $\varepsilon_2 = 4\varepsilon_0$, and $\mu_1 = \mu_2$.

9.2d Demonstrate that Eq. 9.2(4) has a solution for arbitrarily small $k_1 d$ for either TE or TM modes in a dielectric slab guide. Show that there is a minimum of $k_1 d$ which increases with m for $m > 0$.

9.2e (i) For the dielectric slab mode with $m = 0$, find the external decay constant α_x for $k_1 d \gg 1$.

(ii) Also find α_x for TE modes with $k_1 d \ll 1$ and compare with the result of part (i).

9.2f If $\varepsilon_1 \gg \varepsilon_2$, very little energy is contained in medium 2, and the boundaries appear like "magnetic shorts"; that is, tangential magnetic field approaches zero at the interface. Show this from the equations for wave reflections and solve for the lowest-order TE mode with such conditions.

9.3a For a TM_{01} wave in a circular waveguide it is desired to insert a blocking impedance for a given frequency. To do this, a section of shorted radial line (Fig. P9.3*a*) is in-

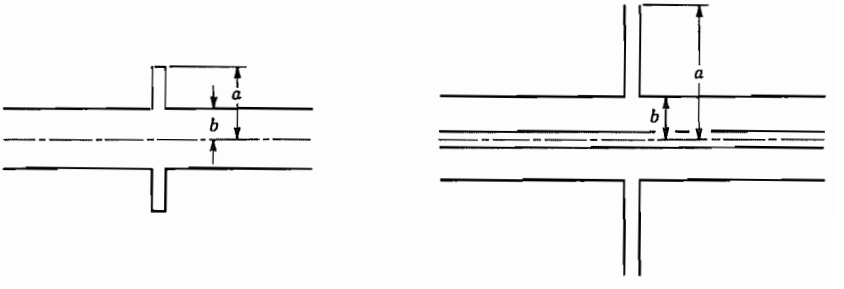

(a) (b)

FIG. P9.3*a*, *b*

[16] *A. Yariv and P. Yeh,* Optical Waves in Crystals, *Sec. 6.4, Wiley, New York, 1984.*

serted in the guide, its outer radius a chosen so that with the guide radius b given, the impedance looking into the radial line is infinite at the given frequency. Suppose that the radius b is 1.25 times greater than cutoff radius at this frequency for the TM_{01} wave and find the radius a.

9.3b It is sometimes required to break the outer conductor of a coaxial line for insulation purposes, without interrupting the rf current flow. This may be accomplished by the radial line as shown (Fig. P9.3*b*) in which a is chosen so that with b and the operating wavelength specified, the radial line has zero input impedance seen from the line. Find the value of a, assuming that end effects are negligible and that $2\pi b/\lambda = 1$.

9.3c Find the voltage at the radius a in terms of the coaxial line's current flowing into the radial line at radius b (Fig. P9.3*b*).

9.3d Taking the classical transmission-line equations with distributed inductance and capacitance varying with radius as appropriate to the radial line,

$$L = \frac{\mu d}{2\pi r} \quad \text{and} \quad C = \frac{2\pi\varepsilon r}{d}$$

Show that the equation for voltage as a function of radius is a Bessel equation, and that the solutions for voltage and current obtained in this manner are consistent with Eqs. 9.3(1) and (2).

9.3e Derive forms similar to Eqs. 9.3(12) and (13) if E_a is specified at r_a, and E_b at r_b. Repeat for H_a specified at r_a, and H_b at r_b.

9.3f For a lossy radial transmission line, find series resistance per unit radial distance (assuming skin-effect condition) for a conductor of surface resistance R_s. Also find shunt conductance per unit radial distance for a dielectric with complex permittivity $\varepsilon' - j\varepsilon''$. Add these to the transmission-line equations (Prob. 9.3d) and obtain the differential equation for voltage.

9.4a Sketch lines of current flow for a circumferential mode with $\nu = 1$ in a radial line of Sec. 9.4. (Take $Z_n = J_n$ for this purpose.) Suggest methods of suppressing this mode by judicious cuts without disturbing the symmetric mode.

9.4b A section of the wedge-shaped guide as in Fig. 9.4*a* may be used to join two waveguides of the same height but different width, both propagating the TE_{10} mode, and a good degree of match is obtained by the process so long as the transition is gradual. Suppose the smaller rectangular guide has $b/a = \frac{1}{2}$ (Fig. 8.7*a*) and the width a_1 of the smaller guide is such that $(f_c)_{TE_{10}} = f/1.2$. The larger guide has the same height and $(f_c)_{TE_{20}} = f/0.8$. Evaluate the wave impedances of the TE_{10} modes in both guides and compare with those in the sectoral horn at the junctions to the rectangular guides, using data of Fig. 9.4*b* for a wedge angle of 20°. Frequency is 10 GHz.

9.5a In the use of the inclined plane line for matching as discussed in Sec. 9.5, suppose that $f = 3$ GHz, $d_1 = 1$ cm, $d_2 = 2$ cm, $kr_1 = 2.5$, and the dielectric is air. If the line to the right is perfectly matched, obtain the approximate standing wave ratio in the line to the left. Compare with that which would exist with a sudden transition, considering only the discontinuity of characteristic impedance.

9.5b Apply the principle of duality to the TE_{11}, TE_{01}, and TM_{01} modes in circular cylindrical waveguides to obtain qualitatively the fields of the "dual" modes. For which of these might boundary conditions be supplied, allowing changes in the conductor position or shape from those of the original mode?

9.5c A wedge-shaped dielectric region is bounded by conducting planes at $\phi = 0$ and ϕ_0,

$z = 0$ and d. Find the field components of the lowest-order mode with E_ϕ, H_r, and H_z. Is this the dual of the mode discussed for sectoral horns in Sec. 9.4?

9.5d Discuss the application of the mode of Prob. 9.5c to the matching between rectangular waveguides of different height, both propagating the TE_{10} mode, describing how to use the solution of Prob. 9.5c to estimate reflections and the approximations involved.

9.5e Show that if kr_1 and kr_2 in the inclined planes of Fig. 9.5 are both large, a matched parallel-plane transmission line with wave impedance η at r_1 gives the same η at r_2, so that a parallel-plane line at that position would also be matched.

9.6a Find expressions for the voltage, current, and characteristic impedance for the principal waves on a transmission line consisting of two coaxial, common-apex cones of unequal angles.

9.6b Write the dual of the mode studied in Sec. 9.6. Can it be supported by physical boundaries using perfect conductors?

9.6c One point of view toward a cylindrical conductor excited by a source across a gap at $z = 0$ (Fig. P9.6c) is that it is a nonuniform transmission line propagating effects away from the gap. (This point of view is used in one theory of cylindrical antennas to be presented in Sec. 12.25.) That is, an elemental section at z may be considered as a biconical line passing through radius a at z. Write the expression for characteristic impedance as a function of z and plot versus z/a for air dielectric.

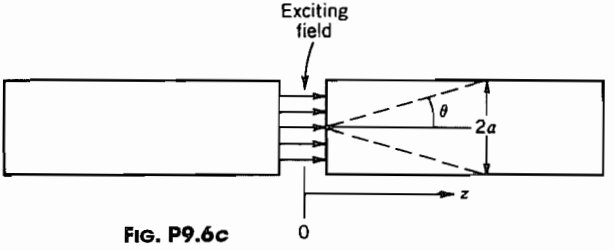

FIG. P9.6c

9.6d For the biconical line of Fig. 9.6, find a capacitance per unit length at radius r based upon charge per unit length along the cones and voltage as defined in Sec. 9.6. Similarly, find an inductance per unit length based upon current at r and the magnetic flux between concentric spheres at r and $r + dr$. Then check velocity $(LC)^{-1/2}$ and characteristic impedance $(L/C)^{1/2}$.

9.6e For a lossy biconical guide, find series resistance per unit length (assuming skin-effect conditions) for a conductor of surface resistance R_s. Also, find shunt conductance per unit length for a dielectric with complex permittivity $\varepsilon' - j\varepsilon''$.

9.7a As a demonstration of the technique of finding cutoff frequencies by calculating transverse resonant frequency, find the cutoff of a TM_{01} mode in circular guide as the resonance of a radial line mode.

9.7b For a TE mode in the small-gap ridge waveguide, the energy stored in electric fields is predominantly in the gap region. If electric field is assumed uniform at E_0 over this region, estimate the stored electric energy u_E per unit length for a single propagating wave in such a guide. If power transfer is $v_g(u_E + u_M)$, and magnetic energy is equal to electric energy, calculate power transfer for a guide with $g = 1$ mm, $2d = 1$ cm, $E_0 = 10^6$ V/m, air dielectric, and operating frequency 1.3 times cutoff frequency.

9.8a Assuming $(v_p/c)^2 \ll 1$, plot kaX/η versus βa for a slow-wave structure. State the requirements on the reactance in order that there may be any slow-wave solution of this type. What should X/η be for βa large?

9.8b Show that a reactance sheet might be used as the boundary condition on fast waves of the TM_{01} type studied in Sec. 8.9. Plot the required value of kaX/η as a function of $k_c a$. Under what conditions might there be a slow wave and a series of fast waves in a given guide of this type?

9.8c** Imagine a parallel-plane transmission line of spacing $2a$ in the x direction, for which both upper and lower planes are cut with many fine straight parallel slits that lie at an angle ψ from the y direction as in Fig. P9.8*c*. Assume no variations with y, and apply approximations as utilized in the helical sheet analysis, obtaining the field components for propagation in the z direction, the complete equation determining β, and the approximate solution of this for $ka \cot \psi \gg 1$.

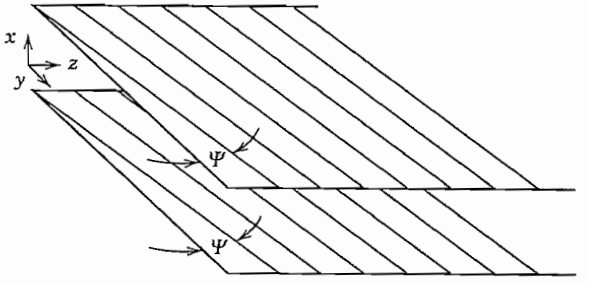

FIG. P9.8c

9.9a Analyze a TE surface wave over a plane with no variations in y and show that a capacitive reactance is necessary to produce an exponential decay with x.

9.9b For the TM surface wave established by the thin dielectric coating on a perfect conductor, find the average power transfer in the z direction. Find the approximate attenuation if the conductor at $x = -d$ has a surface resistance R_s.

9.9c Repeat Prob. 9.9b with a perfect conductor and a dielectric with a small lossy part, $\varepsilon_1 = \varepsilon_1' - j\varepsilon_1''$ with $\varepsilon_1'' \ll \varepsilon_1'$.

9.9d It is desired to pass an electron beam 1 mm above the structure in Fig. 9.9*b*. To match the velocity of the electrons, a wave at 18 GHz should travel at 0.1 the speed of light. Design the fins to produce the appropriate impedance at $x = 0$. How much weaker is the field at the beam than at $x = 0$?

9.10a* Making the assumptions that $kl \ll 1$ and $\beta_0 d \ll 1$, plot the lowest-frequency passband for the structure of Fig. 9.10*a*. Plot the curve for all β and state your reasoning.

9.10b* Take the same approximations as in Prob. 9.10a, but assume the "troughs" are open circuited. Find the equivalent lumped-element circuit, the propagation constant of the fundamental, and sketch the ω–β diagram of this wave. Note the fact that the cutoff region includes $\omega = 0$ and frequencies up to some lower cutoff frequency.

9.10c Find the low-frequency portion of the ω–β diagram for a periodic transmission system composed of parallel L–C circuits in both the series and shunt legs. Note that the fundamental spatial harmonic is a backward wave if the resonant frequency of circuit in the series leg is lower than that for the shunt leg.

9.10d The example used in Sec. 9.10 was a closed line. Consider an open region, such as those studied in Sec. 9.9 for surface wave propagation. What regions of the ω–β plot will represent nonradiating or guided surface waves?

9.10e Illustrate Prob. 9.10d by solving a problem with the structure at $x = 0$ as in Fig. 9.10*a* but with the top plate removed so that the region extends to infinity.